Proceedings of the International Congress on Advances in Applied Physics and Materials Science, Antalya 2011

Models for the Analysis of IR Reflectivity in $TlBiTe_2$ with Different Size of Twins

E. Hatzikraniotis

Department of Physics, Aristotle University of Thessaloniki, 54123 Thessaloniki, Greece

In this work $TlBiTe_2$ were grown by a modified Bridgman technique and examined samples had different lateral dimensions of twins, ranging from 0.1 μm to 1 μm. The average lateral size of the twins seems to affect free carrier concentration and plasma frequency. Infrared spectra were analyzed by two models, the extended Drude model and a generalized empirical model of frequency-dependent damping factor. Increase in size of twins affects the electronic properties and hence plasma reflectivity and free carrier concentration of $TlBiTe_2$.

PACS: 78.20.Bh, 78.30.–j

1. Introduction

$TlBiTe_2$ is a narrow gap semiconductor, which belongs to the family of pseudo IV–VI semiconductors. Since the 1970s, it has been proposed as a candidate material for thermoelectric applications [1] and more recently as a topological insulator [2]. A topological insulator is a band insulator which is characterized by a topological number and which has gapless excitations at its boundaries [3]. The mechanism for the topological insulating behavior in these 3D materials is the band inversion at the Γ point caused by large spin–orbit coupling. The most striking property of this new class of topological insulators is the superconductivity observed in p-doped $TlBiTe_2$ [4].

$TlBiTe_2$ exhibits a phase transformation from the rhombohedral (D_{3d}, low temperature phase) to the cubic (O_h, high temperature phase) symmetry [5], it has been studied by differential scanning calorimetry [6]. As is known [5], rowing the crystal from the melt (the Bridgman method), a cubic phase of a NaCl-type structure is firstly formed. This means that Tl and Bi atoms occupy arbitrarily the one (of the two) fcc lattice sites. During cooling the material is transformed to a rhombohedral lattice that is achieved by an elongation of the [111] direction of cubic lattice. The strain during the transformation from the high temperature cubic phase to the low temperature rhombohedral phase is relieved by the formation of lenticular dislocations and low angle boundaries. As the starting points of the transformation, within the cubic lattice, are more than one (cubic lattice has four equivalent [111] directions), the orientation relationships under which the transformed crystallites can meet each other are three, leading to three different types of twins, which are the coherent {100} and {110} types and the semicoherent {100} (Fig. 1).

In this work, there are compared results for analysis of IR reflectivity vs. growing conditions in $TlBiTe_2$.

2. Experimental

Single crystalline ingots of $TlBiTe_2$ were grown by a modified Bridgman technique. Details on growth conditions are reported elsewhere [7]. Samples of four ingots were examined in this present study, namely, two as grown and two annealed. All four examined ingots had different lateral dimensions of twins, ranging from 0.1 μm to 1 μm.

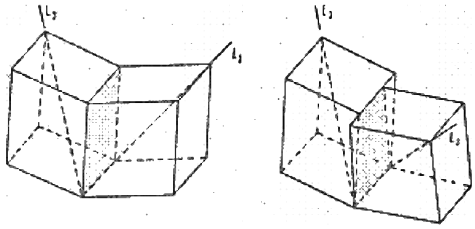

Fig. 1. Types of twins in $TlBiTe_2$.

Samples used in this study were cut from ingots in the shape of circular discs, 9 mm in diameter and 1 mm of thickness, cut perpendicular to the c-axis. Samples were etched and polished for infrared (IR) reflectivity measurements. Etching process was described in detail elsewhere [8].

IR reflectivity measurements were performed at room temperature using a Perkin-Elmer-180 spectrometer in the $E \perp c$ configuration, at the spectral range from 300 cm^{-1} to 3600 cm^{-1}. A wire grid was used as polarizing medium for the measurements. A freshly evaporated Au plate was used as reference.

The Hall effect measurements were carried out at room temperature, using 1.2 T magnetic field in the van der Pauw configuration [9]. Contacts were made by Ag paint.

3. Results and discussion

Results from IR are presented in Fig. 2. Spectra are shifted vertically for clarity. The main characteristic of IR spectra is that they are dominated by a structureless plasmon, with no clear indication for reststrahlen modes. IR reflectivity, $R(\omega)$, is expressed through the complex dielectric function $\varepsilon(\omega)$ as

$$R(\omega) = \left| \frac{\sqrt{\varepsilon(\omega)} - 1}{\sqrt{\varepsilon(\omega)} + 1} \right|^2 \tag{1}$$

and the Drude expression for the complex dielectric function is

$$\varepsilon(\omega) = \varepsilon_1(\omega) + \mathrm{i}\varepsilon_2(\omega) = \varepsilon_\infty - \frac{\varepsilon_\infty \omega_\mathrm{P}^2}{\omega^2 + \mathrm{i}\gamma_\mathrm{P}\omega}\,, \tag{2}$$

where $\varepsilon_1(\omega)$ and $\varepsilon_2(\omega)$ are the real and imaginary part for the complex dielectric function, ε_∞ is the high frequency contribution, ω_P is the plasma frequency, and γ_P is the carrier damping factor. In the classical Drude model ω_P and γ_P are considered as being frequency independent. Previously reported attempts to fit IR reflectivity spectra in $TlBiTe_2$ using various parameters for ω_P and γ_P have been unsuccessful [10].

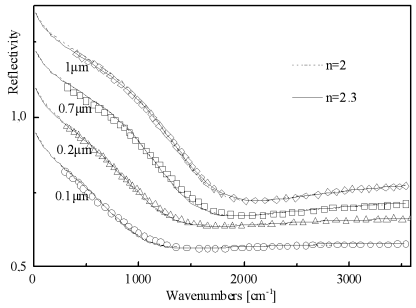

Fig. 2. IR reflectivity spectra for different twin sizes. Solid and dotted lines correspond to different models.

Gervais [11] has extended the simple Drude model, to account for variable damping factor $\gamma_\mathrm{P}(\omega)$. In the extended Drude model, the complex dielectric function is expressed as

$$\varepsilon(\omega) = \varepsilon_\infty - \frac{\varepsilon_\infty \omega_\mathrm{P}^2 - \mathrm{i}(\gamma_\mathrm{P} - \gamma_0)\omega}{\omega^2 + \mathrm{i}\gamma_0\omega}\,, \tag{3}$$

where γ_0 is the damping at $\omega = 0$ and γ_P is the dumping at $\omega = \omega_\mathrm{P}$. Obviously, Eq. (3) turns into Eq. (2) if $\gamma_\mathrm{P} = \gamma_0$. Recently, the extended Drude model has been employed for the analysis of IR reflectivity in $Tl(Bi_xSb_{1-x})Te_2$ compounds [12]. The expression in Eq. (3) is equivalent the classical Drude model (Eq. (2)) taking a frequency dependant $\gamma_\mathrm{P} = \gamma_\mathrm{P}(\omega)$. In fact, from Eq. (2) we may write γ_P as

$$\gamma_\mathrm{P} = \frac{-\omega\varepsilon_2(\omega)}{\varepsilon_1(\omega) - \varepsilon_\infty}\,. \tag{4}$$

Using Eq. (4) and the extended Drude model proposed by Gervais, the frequency dependent $\gamma_\mathrm{P}(\omega)$ is determined as

$$\gamma_\mathrm{P}(\omega) = \frac{\varepsilon_\infty \omega_\mathrm{P}^2}{\varepsilon_\infty \omega_\mathrm{P}^2 + (\gamma_\mathrm{P} - \gamma_0)\gamma_0}\gamma_0 + \frac{\gamma_\mathrm{P} - \gamma_0}{\varepsilon_\infty \omega_\mathrm{P}^2 + (\gamma_\mathrm{P} - \gamma_0)\gamma_0}\omega^2, \tag{5}$$

which reveals to be a quadratic dependence of $\gamma_\mathrm{P}(\omega)$ on ω variable. Assuming that $\varepsilon_\infty\omega_\mathrm{P}^2 \gg \gamma_0(\gamma_\mathrm{P} - \gamma_0)$, which means that the plasmon is not strongly overdamped, Eq. (5) may reduce to a much simpler form, as

$$\gamma_\mathrm{P}(\omega) = \gamma_0 + \frac{\gamma_\mathrm{P} - \gamma_0}{\varepsilon_\infty \omega_\mathrm{P}^2}\omega^2, \tag{6}$$

which actually confirms the definition of γ_0 and γ_P, namely, γ_0 is the damping factor at $\omega = 0$ and γ_P is the dumping factor at $\omega = \omega_\mathrm{P}$. Siapkas [13] and Paraskevopoulos [10] generalized the quadratic expression, for the frequency dependence of $\gamma_\mathrm{P}(\omega)$ derived from Gervais' extended Drude model, using the empirical expression of the form

$$\gamma_\mathrm{P}(\omega) = \gamma_0 + \delta\gamma\omega^n, \tag{7}$$

where the value of the exponent n is close to 2. In fact, the value of exponent n was found to be 2.3 for the case of $TlBiTe_2$ [10].

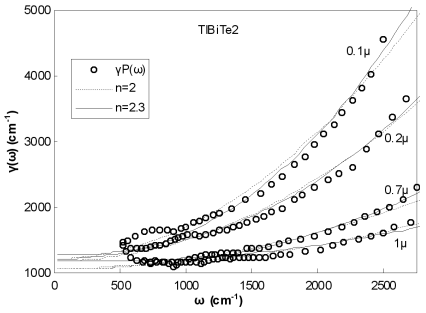

Fig. 3. Calculated damping factor for different twin sizes. Solid and dashed lines correspond to different models.

In this work, there are compared the results for analysis of IR reflectivity vs. the average lateral size of the twins in $TlBiTe_2$. For the analysis, the two above-mentioned models, namely the extended Drude model (Eq. (3)) and the generalized empirical model (Eq. (7)) were used. Results are shown in Figs. 2 and 3. Dotted lines represent the extended Drude model, while solid lines represent fitting with the generalized empirical model. $\gamma_\mathrm{P}(\omega)$ in Fig. 3, was derived from reflectivity data, using the Kramers–Kronig analysis to obtain $\varepsilon_1(\omega)$ and $\varepsilon_2(\omega)$. The Kramers–Kronig algorithm was optimized for improved accuracy at the high and low frequency edge.

In general, both models give very good fitting results, and are practically indistinguishable in reflectivity spectra as shown in Fig. 2. Similarly, the $\gamma(\omega)$ dependence is equally well fitted by the two models, with the generalized empirical being slightly better in high wave numbers (Fig. 2).

Plasma frequency values for the two models vs. average lateral size of the twins are shown in Fig. 4. As can be seen, for both models the values of ω_P are practically the same. Plasma frequency is found increased as the average lateral size of the twins is increased.

The Hall effect measurements revealed that all samples were invariably of *n*-type. Growth conditions and annealing process seem to have a strong effect in the free

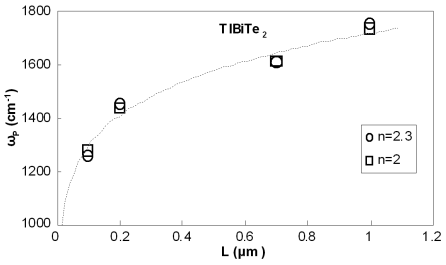

Fig. 4. Calculated plasma frequency (ω_P) for different twin sizes.

carrier concentration. Increasing the average lateral size of twins, an increase is observed in the free carrier concentration, as is evident from Fig. 5.

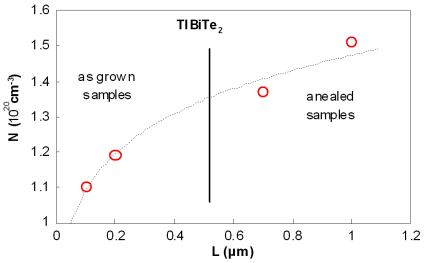

Fig. 5. Free carrier concentration (n) for different twin sizes.

Recently, Hoang and Mahandi, have performed band structure calculations on III–V–VII2 ternary chalcogenides [14], and according to them, there is a highly directional hybridization between the trivalent cation (Sb and Bi), anion (S, Se, Te) and Tl p states. The ordering on the cation sublattice is found to play an important role on the electronic structure of these compounds, and hence increase the plasma frequency and free carrier concentration.

Electrical measurements indicate a transformation from a highly anisotropic to an isotropic structure at 672 K with a sudden jump in the number of carriers [5]. The number of carriers released agrees well with the estimated number of the dangling bond atoms. In annealing, we observe the average size of twins to be increased, which decreases the concentration of dangling bonds and hence increases the free carriers. The ordering of Tl and Bi atoms, which leads to a superstructure is easily detectable by electron diffraction [6], as well as the increase in size of twins affects the electronic properties and hence plasma reflectivity and free carrier concentration in $TlBiTe_2$.

4. Conclusions

In this work, $TlBiTe_2$ were grown by a modified Bridgman technique. Examined samples had different lateral dimensions of twins, ranging from 0.1 μm to 1 μm. The Hall effect measurements were carried out at room temperature. Increasing the average lateral size of twins, an increase is observed in the free carrier concentration ranging from 1.1×10^{20} cm^{-3} to 1.5×10^{20} cm^{-3}. IR reflectivity measurements were performed at room temperature in the $E \perp c$ configuration, at the spectral range from 300 cm^{-1} to 3600 cm^{-1}. IR spectra are dominated by a structureless plasmon, with no clear indication for reststrahlen modes. Plasmon minimum was found increased as the average lateral size of the twins is increased. IR spectra were analyzed by two models, the extended Drude model and a generalized empirical model of frequency-dependent damping factor, $\gamma(\omega)$. Both models seem to fit equally well the reflectivity spectra; however, the generalized empirical model gives a slightly better fitting in the high wave numbers region for the damping factor, $\gamma(\omega)$. Evaluated plasma frequency values, were practically the same for the two models and were found increased as the average lateral size of the twins is increased. The ordering of Tl and Bi atoms leads to a superstructure easily detectable by electron diffraction. Atom ordering, and also the increase in size of twins, seems to have an influence on the electronic properties and hence affect the plasma reflectivity and the free carrier concentration in $TlBiTe_2$.

References

[1] L.G. Voinova, V.A. Bazakutsa, S.A. Dembovskii, L.G. Lisovskii, E.P. Sokol, Ch.T. Kantser, *Izv. Vys. Uchebn. Zav., Fizika* **5**, 154 (1971) (in Russian).

[2] B. Yan, Ch.-X. Liu, H.-J. Zhang, Ch.-Y. Yam, X.-L. Qi, Th. Frauenheim, Sh.-Ch. Zhang, *Europ. Phys. Lett.* **90**, 37002 (2010).

[3] X.-L. Qi, S.-C. Zhang, *Physics Today* **63**, 33 (2010).

[4] R. Hein, E. Swiggard, *Phys. Rev. Lett.* **24**, 53 (1970).

[5] O. Valasiades, E.K. Polychroniades, J. Stoemenos, N.A. Economou, *Phys. Status Solidi A* **65**, 215 (1981).

[6] K. Chrissafis, E.S. Vinga, K.M. Paraskevopoulos, E.K. Polychroniadis, *Phys. Status Solidi A* **196**, 515 (2003).

[7] E.K. Polychroniadis, J. Stoemenos, *J. Cryst. Growth* **55**, 388 (1981).

[8] E.K. Polychroniadis, J. Stoemenos, *J. Mater. Sci.* **17**, 2077 (1982).

[9] L.J. van der Pauw, *Philips Res. Rep.* **13**, 1 (1958).

[10] K.M. Paraskevopoulos, D. Siapkas, N.A. Economou, *Phys. Status Solidi* **124**, 229 (1984).

[11] F. Gervais, *Mater. Sci. Eng.* **39**, 29 (2002).

[12] K.M. Paraskevopoulos, E. Hatzikraniotis, E.S. Vinga, M. Ozer, A. Anagnostopoulos, E.K. Polychroniadis, *J. Alloys Comp.* **467**, 65 (2009).

[13] D. Siapkas, *Sci. Ann. Fac. Phys. Math., Univ. Thessaloniki* **20b**, 163 (1980).

[14] K. Hoang, S.D. Mahandi, *Phys. Rev. B* **77**, 205107 (2008).